

Comparison of Stationary Internal Cooling Passage Numerical Simulations to Experimental Data

M. McGilvray¹ - C. Orozco Piñeiro² - T. Axe² - J. Ryley¹ - D.R.H. Gillespie¹

¹Osney Thermo-Fluids Lab, University of Oxford, Oxford, UK

²Rolls-Royce UK, Derby, UK

ABSTRACT

Turbine blade internal cooling analysis is currently improving with a shift from the application of wall averaged empirical correlations to spatially resolved numerical simulations. However, verification of the numerical tools is required before industry would apply and rely upon a more costly tool in the design stage. This paper presents the numerical simulation of a stationary, generalised rib turbulated internal cooling passage with a 1:2 aspect ratio with engine realistic features over a Reynolds range of 18000-112000. Direct comparisons of numerical simulations using both the realizable k- ϵ and k- ω SST turbulence models and experimental results are presented in terms of spatially resolved Nusselt number, streamwise averaged Nusselt number, and wall averaged Nusselt number and friction factor. This showed that similar behaviour, with averaged differences in Nusselt number of 5-30% between the experiment and the simulations, with the end section of the passage being well predicted by the k- ϵ turbulence model. The friction factor agrees well between the two sets of numerical predictions and with the experimental results for Reynolds numbers below 70000 with a maximum under-prediction of 12%. Both turbulence models resulted in similar wall averaged Nusselt numbers, though the best point-wise match with experimental data was Reynolds number dependent.

NOMENCLATURE

A	Area, m ²	y^+	Dimensionless wall distance
c_p	Specific heat at const. p., J/kg.K	z	Streamwise distance, m
$D_h = \frac{4A}{P}$	Hydraulic diameter, m	Greek symbols	
e	Rib height, m	α	Rib angle to z direction
f	Friction factor	μ	Viscosity, Pa.s
HTC/ h	Heat Transfer Coefficient, W/m ² .K	ρ	Density, kg/m ³
I	Turbulence intensity	Subscripts	
k	Thermal conductivity, W/m.K	0	Normalisation
$Nu = \frac{hD_h}{k}$	Nusselt number	<i>gas</i>	Driving gas
p	Transverse position on perimeter, m	<i>m.b.</i>	Mixed bulk
P	Perimeter, m	<i>proj.</i>	Projected area
Pr	Prandtl number	<i>rib</i>	Value on rib
\dot{q}	Heat flux, W/m ²	<i>surf.</i>	Surface area
T	Static temperature, K	<i>wall</i>	At wall
$Re_{D_h} = \frac{\rho W D_h}{\mu}$	Reynolds number		
W	Streamwise velocity, m/s		

INTRODUCTION

Current design practices of HP turbine blade passages for the internal heat transfer still rely upon a combination of empirical correlations for the calculation of wall average heat transfer (Han et al. (2000)) and normalised CFD heat transfer distributions (Jackson et al. (2009)). However, the bulk of these empirical correlations are based upon experimental data taken in idealised passages, with sharp passage corners and ribs, and intake geometries that vary to those seen in real engines (Schüler et al.

(2009)). In the open literature, there is a lack of experimental data on the heat transfer levels on the planar walls. Also, there is little to no validation studies that have verified the accuracy of complete passage heat transfer distributions from numerical calculations using current industrial practices (see Jackson et al. (2009) study of serpentine passages). Therefore, the validity of this design approach is both not documented and can incur large uncertainties.

A series of stationary heat transfer tests were undertaken on an internal cooling passage with realistic filleting features on the passage corners and rib turbulators (Ryley et al. (2013)). The experiments used the transient liquid crystal technique to measure spatially resolved HTC on all the surfaces, with high resolution data taken in the rib turbulator region. The experiments included varying the aspect ratio (only 1:2 aspect ratio passage data presented in this paper) of the passage and mass flow rate of the flow. The experiments used two sets of hybrid ribs, to allow for average HTC to be determined on each individual rib. Additional experiments were undertaken to measure the friction factor.

The experiment was numerically simulated, taking the flow path of the experiment from the heater mesh to the outlet plenum. Meshing of the flow path used ANSYS ICEM CFD 12.1 (ANSYS (2009)), and the numerical simulations used the CFD solver ANSYS Fluent 13.1 (ANSYS (2012)). Industry best practices were applied to model the flow (RANS calculations) and methods used to derive the HTC values. A model parameter sensitivity study was undertaken to quantify the effects modelling choices. Results from these simulations are briefly presented.

This paper compares the numerical simulation results to the experimental data, presenting heat transfer and pressure loss data for a range of Reynolds number cases. This includes evaluating the average Nusselt number levels along the passage, as well as the spatial variation of the Nusselt number distribution. Experimental and numerical data are also compared to empirical correlations currently used in industrial design. Influences of experimental uncertainties and modelling sensitivities are examined.

EXPERIMENTAL SETUP

A brief summary of the experimental rig and passage is described below, with a more detailed description of the experiment and results in the accompanying paper (Ryley et al. (2013)). Figure 1 presents the stationary internal cooling rig, which includes a single pass of a rib turbulated passage. The experiment measures spatially resolved HTC values by using the transient liquid crystal method. Flow is established in the passage at ambient temperature, setting isothermal conditions with the surroundings. The test is initiated with the activation of the heater mesh which creates a rapid change to the gas temperature, causing heat transfer to the passage wall, increasing the surface temperature and altering the colour response of the liquid crystals. The rig is operated in suction mode, with the outlet plenum connected to a vacuum line, where a gate valve is located to set the mass flow rate (measured with an orifice plate on the intake). A flow straightener and baffle plate are located before and after the test section respectively in order to promote flow uniformity through the passage. The heater mesh (50×50 mm) is situated 400 mm upstream of the contoured section to the internal cooling passage. The HTC distribution was measured at five nominal mass flow rates (passage Reynolds numbers): 9.45, 16, 29.5, 50 and 53.2 g/s (18900, 32000, 59000, 100000, 106400). Two tests are performed to measure HTC values on all four walls (which will have slightly different mass flow rates), as instrumentation enters through the rear side wall allowing only three walls to be viewed in a given test.

The internal cooling passage test section consists of a rectangular duct with corner fillets (radius of width/4) with rib turbulators on opposing walls (suction surface and pressure surface, prescribed from 45° of passage fillets) and two smooth side walls (leading edge and trailing edge, prescribed from 45° of passage fillets). The passage width is 18.66 mm and the length of the passage is 432 mm. The aspect ratio (width:height) of the passage is 1:2, with a hydraulic diameter of 26.1 mm (calculated neglecting ribs). Ribs in the passage are: at an angle (α) of 45° to the streamwise direction; have a

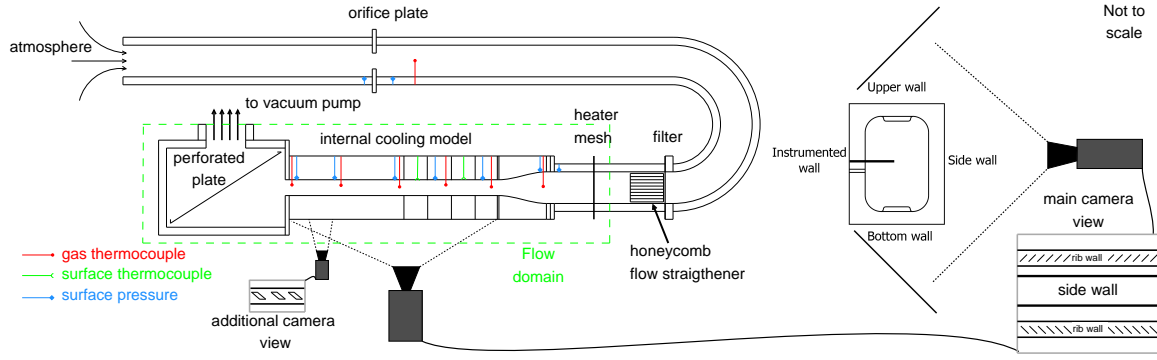


Figure 1: Schematic of experimental setup of flow path, instrumentation and camera view.

spacing (P/e) of 10; are filleted in all three directions (radius of filleting is $e/2$); are centred and span half the width of the passage; and are staggered by half the pitch; rib blockage (e/D_h) of 6.9%.

Five K-type gas thermocouple measurements were taken along the centreline at 41.5, 149.5, 228.5, 298.5 and 419.5 mm from the start of the passage. The experimental HTC values determined are based on a linear interpolation of the centreline gas temperature measurements to each streamwise location. Nusselt numbers are calculated from the HTC distributions, passage hydraulic diameter and the thermal conductivity based on the centreline gas temperature average over the test period and using the same linear interpolation method as the HTC calculation for each streamwise location. HTC values were measured for some of the ribs as an average projected area value, using the hybrid technique (Wang (1991)). In separate tests with no heating and at room temperature, five static pressure measurements (Sensortech HX and BTE, transducer was dependent on pressure level) were measured on the mid plane of the trailing edge wall (42, 150, 261.5, 361.5, 386.5 mm from start of the passage) for 14 mass flow rates. The Fanning friction factor is based on a robust linear fit of the final four pressure measurements, and the density at the second pressure measurement location. Due to entrance effect differences, it was found that a clearer comparison could be made by ignoring the first pressure measurement. Uncertainties for the HTC values were determined at each spatial location using a perturbation method based on evaluating contribution of each experimental measurement uncertainty (further details in Ryley et al. (2013)).

Some of the data presented in this paper is normalised for clearer interpretation of the results. The data (both experimental and numerical) is normalised by the the turbulent, fully developed smooth pipe flow correlations for Nusselt number (Equation 1 - Ditus-Boelter) and friction factor (Equation 2 - Blasius). The Prandtl number is taken as 0.71. When data is presented as singular values (as in Figure 7), the region averaged is the downstream half (216-432 mm) of the passage where the flow is more developed and experimental HTC data exists on the ribs.

$$Nu_0 = 0.023 Re_{D_h}^{0.8} Pr^{0.4} \quad (1)$$

$$f_0 = 0.079 Re_{D_h}^{-0.25} \quad (2)$$

NUMERICAL CALCULATION SETUP

The numerical calculations used in this study apply current industry practises in design and verification of turbine internal cooling passages. The calculations were performed using the ANSYS Fluent 13.1 software (ANSYS (2012)), with a RANS formulation and SIMPLE pressure based solver. As the experimental method is assumed to give the same values of HTC and friction factor as would be measured in steady state, there is no need to model the transient aspect of the experiment. A stepped approach was taken in the calculation, building in complexity to a solution with: green-gauss node based gradient discretisation, standard pressure, second order upwind discretisation for remaining

properties, temperature and pressure dependent density, temperature dependent heat capacity, viscosity, thermal conductivity and turbulence.

The calculations were performed on the flow path from the heater mesh to 50 mm into the outlet plenum to replicate the experimental inflow boundary layer and exhaust conditions. A constant mass flow inlet was applied at the heater mesh location, with a spatially uniform inlet temperature profile of 313 K which roughly estimates what is produced experimentally by the heater mesh. A constant outflow pressure profile of -10 kPa gauge was applied with spatial uniformity. The walls of the passage were modelled as isothermal at a temperature of 293 K, a 20 K difference to the inflow temperature. Simulations were undertaken for seven mass flow rates, the five nominal experimental mass flow rates and at 20 and 40 g/s (passage Reynolds numbers of 40475 and 80950 respectively) to more evenly span the mass flow rate range. Convergence was obtained for all calculations, with residual levels (Fluent default) on the order of magnitude 10^{-5} for continuity, 10^{-6} for momentum, 10^{-7} for energy and 10^{-5} for the turbulence properties.

Turbulence modelling was implemented with two different two equation models: $k-\omega$ SST and the realisable $k-\epsilon$ with near wall enhancement. These models were chosen due to their general application previous internal cooling passage studies (Jackson et al. (2009)). The turbulence kinetic energy and length scale were applied as a turbulence intensity and hydraulic diameter based on the inlet assuming fully developed flow. The intake of the rig has a hydraulic diameter of 50 mm, and the turbulence intensity was calculated using an empirical correlation for fully developed pipe flow (Equation 3 from ANSYS (2012)). Any changes in the turbulent length scales due to the fine porosity of the heater mesh should be washed out well before the internal cooling passage.

$$I = 0.16Re_{D_h}^{-\frac{1}{8}} \quad (3)$$

The mesh was generated using ANSYS ICEM CFD 12.1 (ANSYS (2009)) software, with unstructured tetrahedral elements and a prismatic layer. The same mesh was used in all the simulations, with the mesh through the mid plane of streamwise direction shown in Figure 2. This mesh has a total number of cell count of 3863291, with 2853852 cells in the passage with maximum y^+ values on the tip of the ribs of 0.18 and 0.62 for lowest and highest mass flow rate cases respectively. A mesh independence study was performed by running a simulation with an increase of cells to 8189221. The sensitivity to the mesh was seen to be quite different between the turbulence models: for the realizable $k-\epsilon$ model, the finer mesh reduced the Nusselt number on average by 0.5%, where the largest differences were on the leading edge of 15% due to slight shifting in the extent of the secondary flow impingement. The friction factor shifted by 3.6%; the $k-\omega$ SST model showed a slight increase in the average Nusselt number of 0.3%, however the secondary flow impingement shifts much more downstream and a reduction in the peak Nusselt number of the middle of the passage of up to 20%. The friction factor shifted by 1.5%.

The heat transfer coefficient is post-processed at each element centre location by Equation 4, by exporting the total wall heat flux and relevant gas temperature data. This is remapped into streamwise and transverse (perimeter) positions using a linear interpolation to structured grid of 0.25 mm resolution (same as the experiment and similar cell resolution as calculation), where the rib values are averaged and calculated on the projected area (Equation 5). Three different choices of gas temperature are applied: the centreline gas temperature at each spatial location (within 0.25 mm of true measurement location); an interpolation of the centreline gas temperature using the same method applied to the experimental data, where centreline gas temperatures are taken from the simulation at the five experimental thermocouple locations; an interpolation of the mixed bulk temperature calculated from the simulation data (Equation 6) from the five experimental thermocouple locations. This provides both a direct comparison of experimental and numerical results while also providing a comparison to mixed bulk temperature definition of HTC, which is generally applied in passage design.

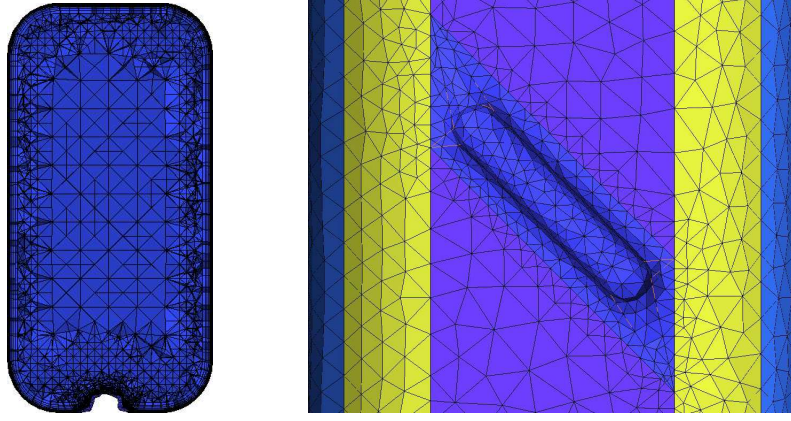


Figure 2: Image of mesh at the mid plane of the streamwise direction (left) and the surface mesh around a rib (right, flow direction up the page).

For the Nusselt number calculation, the thermal conductivity is based on the gas temperature at each spatial location taken for the HTC calculation. Friction factor is based on the same method applied to the experimental data, where a robust linear fit is taken of the pressure for the final four experimental measurement locations on the mid span of the trailing edge wall and the density at the second measurement location.

$$h = \frac{\dot{q}}{T_{gas} - T_{wall}} \quad (4)$$

$$h_{rib} = \frac{\sum (h_{(p,z)} A_{surf.(p,z)})}{\sum A_{proj.(p,z)}} \quad (5)$$

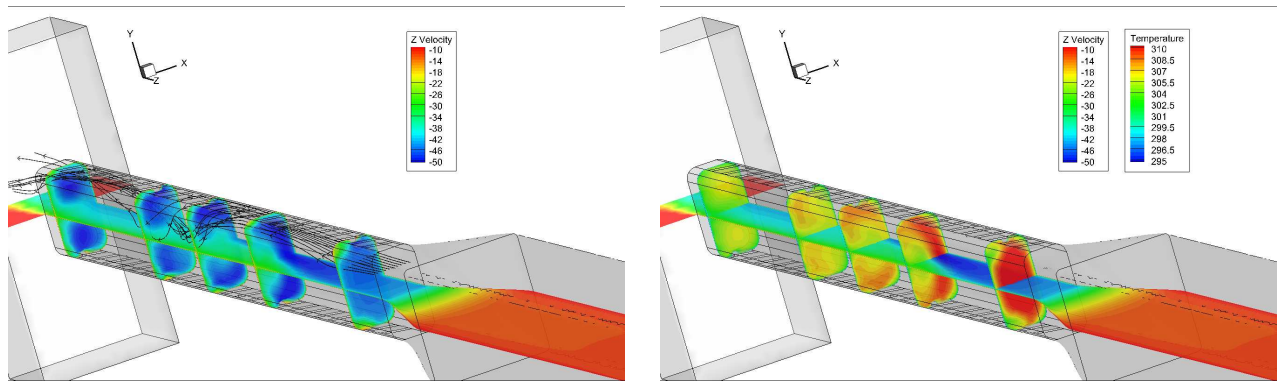
$$T_{m.b.} = \frac{\int \rho W c_p T dA_z}{\int \rho W c_p dA_z} \quad (6)$$

NUMERICAL RESULTS

A brief insight of the results of the numerical calculations is presented in this paper. To give an example of the generalised flow structure that develops in the passage, Figure 3 presents flow information for a Reynolds number of 61,000 $k-\omega$ SST simulation. This firstly shows that the passage does not become fully developed with changes in the temperature and velocity field along the entire length of the passage. This causes the Nusselt number distribution to vary significantly in the streamwise direction. The common double vortex structure is seen to develop in the passage, as evidenced by the streamlines. In the core of the vortex structure, the streamwise velocity and static temperature is at a maximum for the given streamwise location. A peak in Nusselt number on the trailing edge at 225 mm (and actually situated on the mid plane of the passage) is caused by the acceleration of higher temperature gas along this wall as the secondary flow from the first ribs, which has a reduced streamwise velocity, convects into the middle of the passage. A follow on effect from this is seen on the ribbed walls (340 mm), then the leading edge (360 mm) as this hotter/quicker gas moves away from these surfaces, reducing the Nusselt number.

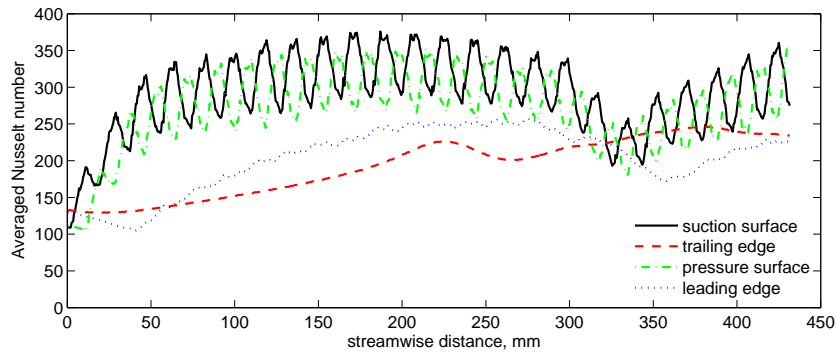
Sensitivity Analysis

Various parameters which required judgement in simulating the experimental tests were explored to quantify the sensitivity of the results. These include: turbulence intensity and length scales; intake duct length; mass flow rate; choice of gas driving temperature. These were investigated numerically



(a) Stramlines and velocity contour planes (m/s) at streamwise thermocouple locations/y mid plane.

(b) Velocity contour on y mid plane (m/s), temperature contour planes (K) at streamwise thermocouple locations.



(c) Streamwise variation of transverse averaged Nusselt number. Calculated using an interpolation of mixed bulk temperature at thermocouple locations.

Figure 3: Flow and heat transfer results from numerical calculation for a nominal Reynolds number of 61,000, for the $k-\omega$ SST turbulence model. Flow right to left, negative z direction.

by taking the 61,000 as the base Reynolds number case (mass flow rate of 29.5 g/s) and the $k-\omega$ model as the base turbulence model.

The sensitivity of the results to the turbulence settings applied was studied numerically as the turbulence intensity and length scales were not measured directly and calculated assuming fully developed pipe flow in the intake. Perturbing the turbulence intensity and the hydraulic diameter (i.e. the turbulent kinetic energy and length scale) by $\pm 10\%$ both caused a similar shift of $\pm 0.02\%$ in average Nusselt number and $\pm 0.015\%$ in friction factor. Therefore, the inflow turbulence properties were found to have minimal impact on the numerical results.

The boundary layer development in the experimental rig would start well before the heater mesh. To investigate the effect of only modelling from the heater mesh, the passage was simulated with an intake duct that was doubled in length, making the length between the inlet and the contoured intake 800 mm. The mesh was rebuilt using the same properties applied to generate the standard mesh used in this study. Overall, the flow structure was seen to shift further upstream with a difference in the average Nusselt number of -2.5% and friction factor of 2.2% . However, a large increase in Nusselt number occurs in the first 150 mm of the model, requiring a balanced drop in Nusselt number downstream where data is used in averaging the heat transfer data. This will have a significant impact on direct comparison of the numerical and experimental results spatially, though may not impact greatly on average values.

The mass flow rate that was measured experimentally had an accuracy level around $\pm 1\%$. Perturbing the inflow mass flow rate by this amount, the average Nusselt number was seen to change by $\pm 0.7\%$ and friction factor by $\pm 0.1\%$ and this change was seen to be fairly even across the entire surface. This is similar change to that predicted by empirical correlations of Han et al. (1989) and

smooth pipe correlations for fully developed turbulent pipe flow. The sensitivity of the results to mass flow rate is quite small in comparison to other sensitivities and experimental uncertainties.

In the design of internal cooling passages, the usual practice is to base the driving gas temperature on the mixed bulk temperature. As the experimental method does not allow for this to be measured directly without significant disruption of the flow, the HTC is based on centreline gas temperature measurements. As shown in Figure 4, there is quite a significant difference in the centreline to mixed bulk temperature in the initial part of the passage, as also seen in the contour plots in Figure 3. The difference in driving gas temperature to wall temperature varies by a peak of 26.4% at 150 mm in the passage (directly related to Nusselt number difference), while the average Nusselt number only shifts by 2%. Thus, care should be taken in comparing results produced using different approaches.

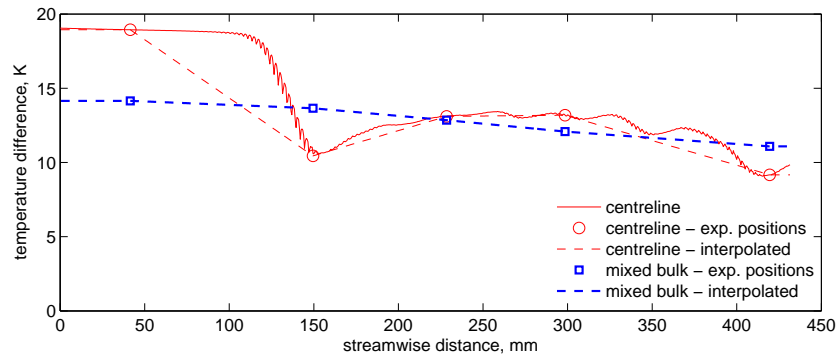


Figure 4: **Different gas temperatures profiles used in the calculation of the numerical simulation Nusselt number (Reynolds number of 61,000 simulation and $k-\omega$ SST turbulence model).**

COMPARISON OF NUMERICAL TO EXPERIMENTAL RESULTS

Figure 5 presents a direct comparison of the Reynolds number of 61,000 Nusselt number distributions (driving gas temperature based on interpolated centreline) between experiment and both numerical calculations. Further notes on the nomenclature and unwrapping method can be found in the accompanying paper (Riley et al. (2013)). Overall, most of the key features seen experimentally are captured well in both numerical simulations: highest heat transfer on the ribs, then in the flow reattachment region behind each ribs; streaks of high Nusselt number produced by secondary flows on the leading edge; streamwise variation of Nusselt number. The Nusselt number in the numerical calculations where the secondary flow impinges the passage fillet is similar to the experimental case although the high Nusselt number streaks experimentally appear at an angle closer to the streamwise direction. With the experimental uncertainty in this region similar to that on leading edge of 8.9%, this suggests the radial correction applied due to two-dimensional conduction (Riley et al. (2013)) is applicable. Overall, the realizable $k-\epsilon$ model has lower spatial differences and overall Nusselt number than the $k-\omega$ simulation. With consideration of the experimental uncertainty (average is 7.9%, peak in regions up to 18%) and sensitivities of the simulation parameters (up to 5% on average, and regions which peak up to 25%), the numerical results give a reasonable reflection of the experiment.

To make a more direct comparison between the experiments and numerical simulations, Figure 6 presents the streamwise average of Nusselt number on all four walls. This comparison can highlight the true difference while avoiding the miss-representation of small spatial shifts in peaks/troughs of the Nusselt number that will have minimal effect in an engine due to high conduction rates. Overall, both numerical simulations do a reasonable job at predicting the experimental measurements in the context of the experimental accuracy and modelling sensitivities. The $k-\epsilon$ turbulence model more closely reflects the experimental data, especially in the final 100 mm of the passage where the flow is more fully developed. The $k-\omega$ model appears to over-estimate the strength of the secondary flow, with high HTC regions on where these regions impact the leading edge.

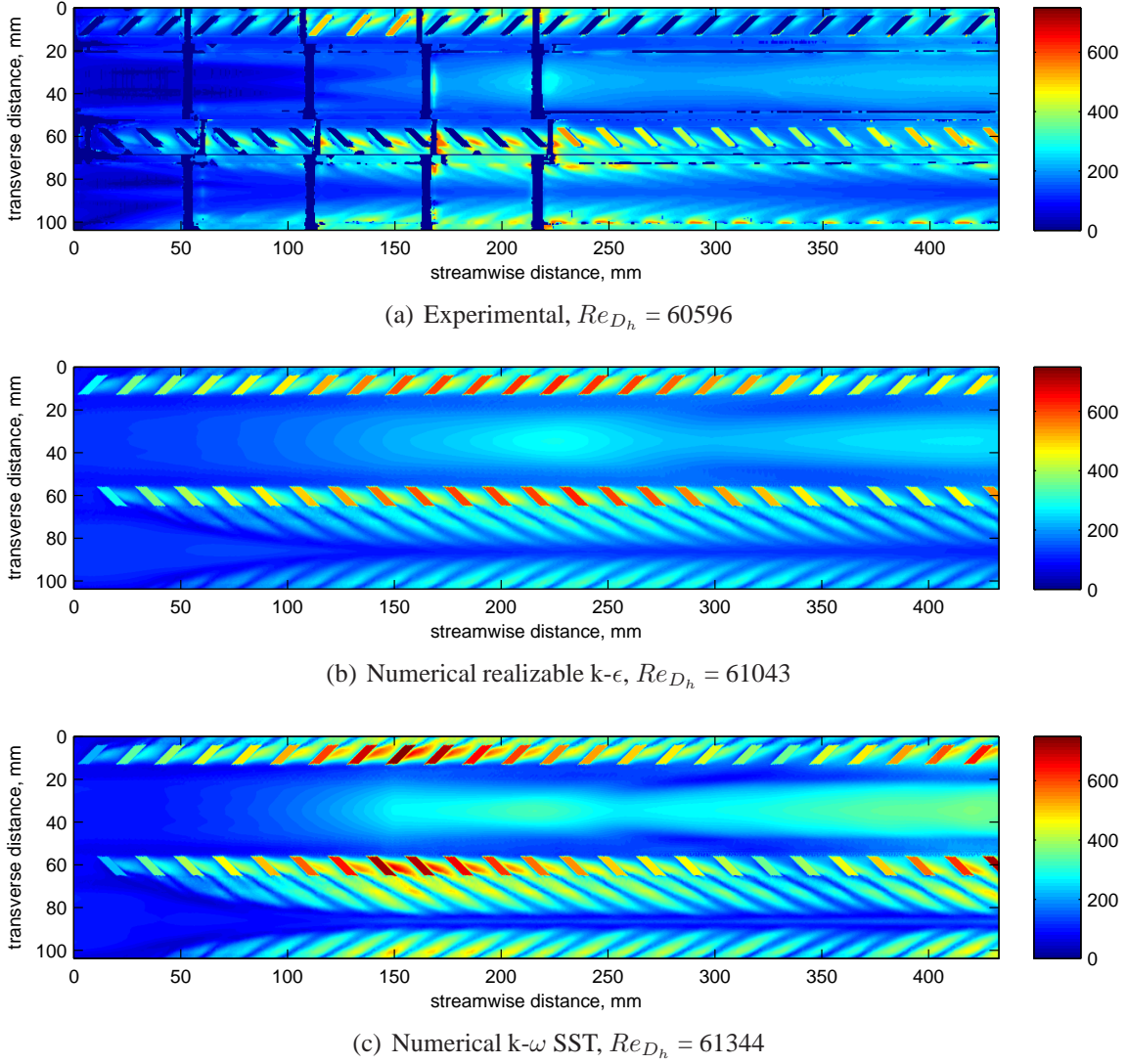


Figure 5: Comparison of Nusselt number distributions between experiment and calculations for a nominal Reynolds number of 61,000. Driving gas temperature taken as an interpolation between experimental thermocouple locations on the passage centreline.

A comparison between the experiments and the two numerical calculations is presented of the averaged normalised Nusselt number (total, ribbed walls, side walls) and friction factor as a function of Reynolds number (Figure 7). As the flow is not fully developed and the peaks and troughs in Nusselt number are at different streamwise locations in the two sets of simulations and experiments, this comparison is limited but still insightful. The data is also compared to the empirical correlations developed for sharp edge rib passages of Han et al. (1989) and rounded edge rib passages of Rallabandi et al. (2011). These give a benchmark to which industry currently uses in design, though are not directly comparable (the merits of the correlations are discussed in detail in the companion paper (Ryley et al. (2013))).

The normalised friction factor for both numerical simulations is in close agreement for the full range of Reynolds numbers. The two numerical simulations agree with the experimental measurements at Reynolds numbers below 70000, though show an under-prediction of normalised friction factor at large Reynolds numbers, with a maximum of 12% at a Reynolds number of 112000. As the sensitivity of friction factor to simulation parameters at a Reynolds number of 60000 was a maximum of 2.5%, there is no obvious reason for this diversion. The data is seen to be fairly similar to the sharp rib correlation, especially for Reynolds numbers between 40000-90000.

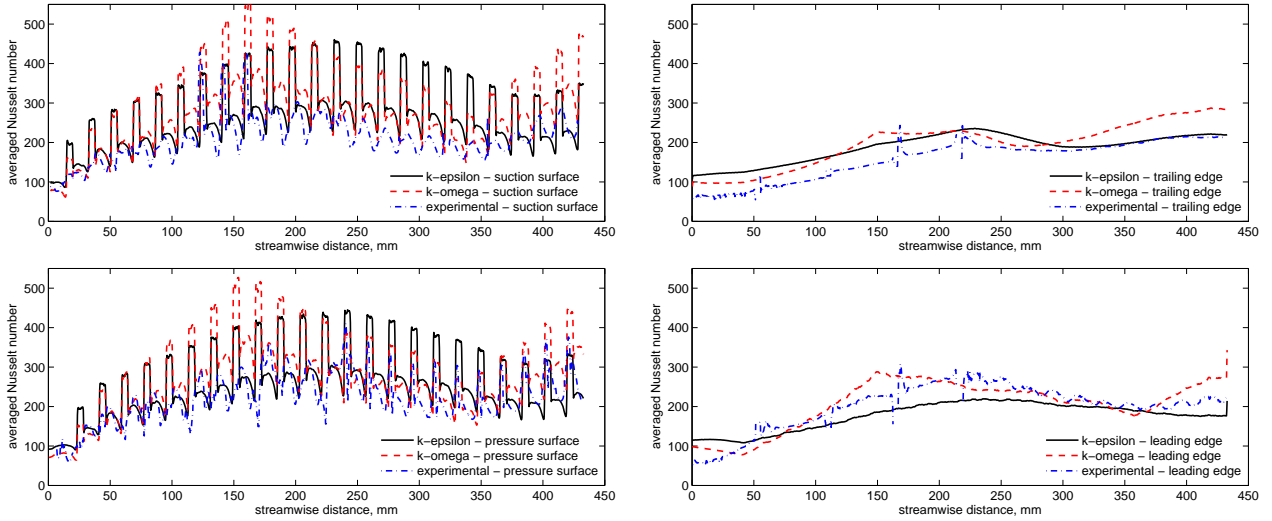


Figure 6: Comparison of streamwise variation of transverse averaged Nusselt number for a nominal Reynolds number of 61,000 for each wall. Driving gas temperature taken as an interpolation between experimental thermocouple locations on the passage centreline. Ribbed wall data averaged at rib angle. Experimental data on ribs only shown for hybrid ribs.

Overall, the difference in average normalised Nusselt number on all walls between the experiment and the realizable $k-\epsilon$ model is less than 15% for all cases. Only for low Reynolds numbers on the pressure surface does the $k-\omega$ SST simulation obtain results closer to the experiment. At high Reynolds numbers, both numerical solutions have higher normalised Nusselt numbers on all walls except the leading edge. The numerical average normalised Nusselt number for the pressure surface are similar to both correlations (within 10%), though show a different trend at higher Reynolds numbers to both the correlations and the experimental data which both continue to decrease. This behaviour could be an artifact of the flow not being fully developed in the region used for averaging. The side walls have a constant enhancement over turbulent, fully developed smooth pipe flow with relation to Reynolds number, with the leading edge being 1.65 times larger and the trailing edge 1.4 times larger.

CONCLUSIONS

This paper has summarised comparisons between experimental measurements and numerical predictions of heat transfer and flow losses in a 1:2 internal cooling passage with engine realistic features over a Reynolds number range of 18000-112000. By performing a numerical sensitivity study and with the measurements of Nusselt number being spatially resolved, the comparisons between experiments and numerical predictions highlight the importance of the presumption of fully developed flow and influences of the intake on flow losses and heat transfer. Overall, reasonable agreement was found between the experiments and the numerical predictions with average Nusselt numbers being over-predicted by 5-30%. The friction factor showed very good agreement for Reynolds numbers below 70000, with a maximum under-prediction of 12% at the highest Reynolds number of 112000. The differences between the turbulence models applied was small in terms of wall averaged heat transfer and friction factor, though point wise agreement was highly case dependent.

ACKNOWLEDGEMENTS

This research received funding from the European Union Seventh Framework Programme (FP7/2007-2013) under grant agreement no. 233799 (ERICKA). The authors acknowledge the contributions to this work from Trevor Godfrey, Gerald Walker, Dave Mountain, Bharat Lad and EDM.

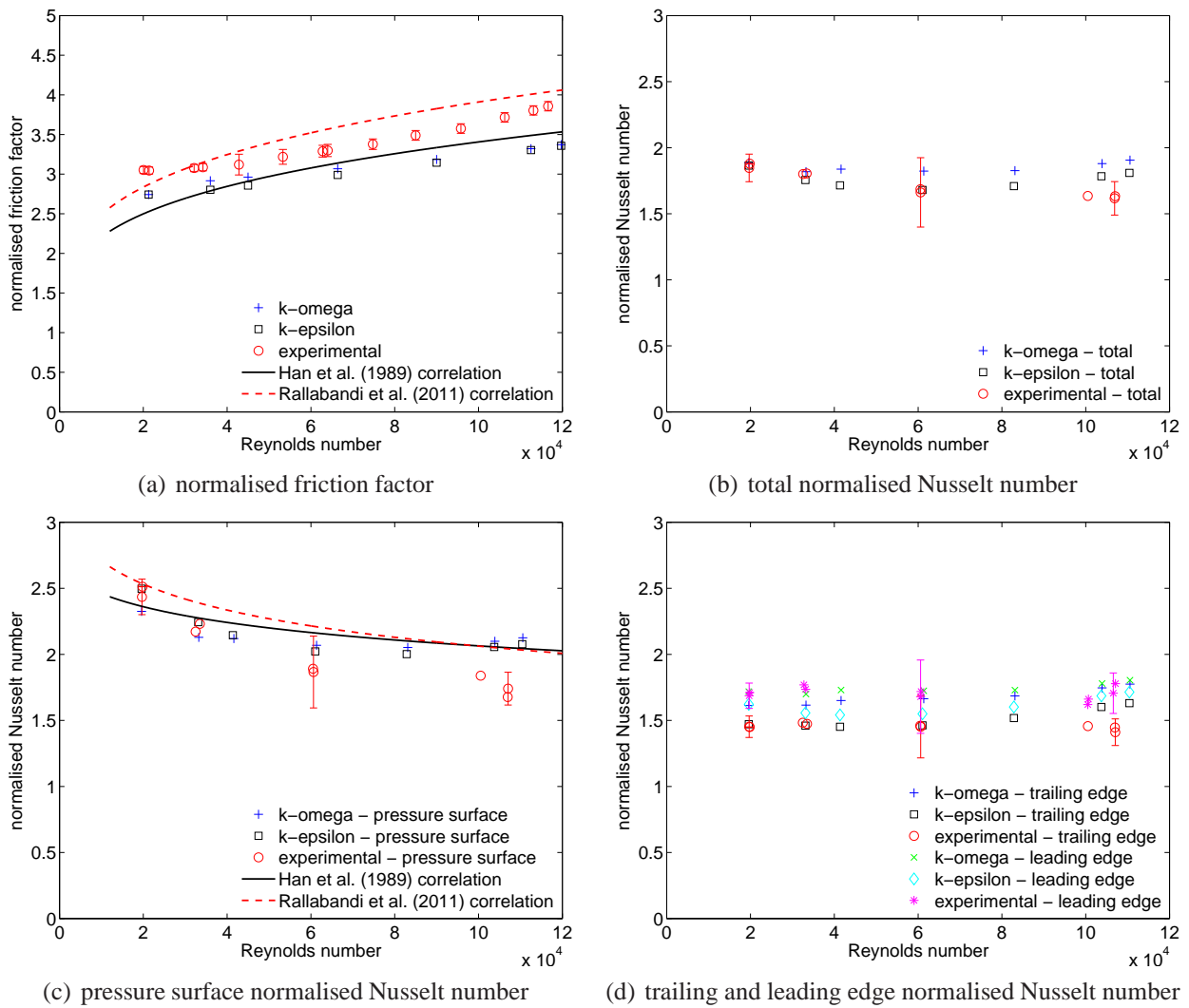


Figure 7: Comparison of normalised friction factor and area averaged normalised Nusselt number over different walls between the numerical calculations and experiments over the range of Reynolds numbers. Average taken between 216-432 mm in streamwise direction.

REFERENCES

- ANSYS (2009). ANSYS ICEM CFD 12.0 User Guide. Technical report, PathScale Corporation.
- ANSYS (2012). ANSYS Fluent 13.1 User Guide. Technical report, PathScale Corporation.
- Han, J., Dutta, S., and Ekkad, S. (2000). *Gas Turbine Heat Transfer and Cooling Technology*. Taylor and Francis. ISBN: 15603284.
- Han, J., Ou, S., Park, J., and Lei, C. (1989). Augmented heat transfer in rectangular channels of narrow aspect ratios with rib turbulators. *International Journal of Heat and Mass Transfer*, 32(9):1619–1630.
- Jackson, D., Ireland, P., and Cheong, B. (2009). Combined experimental and CFD study of HP blade multi-pass cooling system. *Proceedings of ASME Turbo Expo 2009; Power for Land, Sea and Air*, (GT2009-60070).
- Rallabandi, A. P., Alkhamis, N., and Han, J. (2011). Heat Transfer and Pressure Drop Measurements for a Square Channel With 45 deg Round-Edged Ribs at High Reynolds Numbers. *Journal of Turbomachinery*, 133.
- Ryley, J., McGilvray, M., and Gillispie, D. (2013). Stationary internal cooling passage experiments for an engine realistic configuration. *10th European Conference on Turbomachinery, Fluid Dynamics and Thermodynamics*.
- Schüler, M., Neumann, S. O., and Weigand, B. (2009). Pressure loss and heat transfer in a 180 deg bend of a ribbed two-pass internal cooling channel with engine-similar cross sections, part 1: Experimental investigations. *8th European Conference on Turbomachinery, Fluid Dynamics and Thermodynamics*, (ETC8-115).
- Wang, Z. (1991). *The Application of Thermochromic Liquid Crystals to Detailed Turbine Blade Measurements*. PhD thesis, University of Oxford.